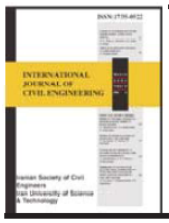

International Journal of Civil Engineering

Structure-Earthquake

Nonlinear dynamic analysis of concrete gravity dams considering rotational component of ground motion

L. Kalani Sarokolayi[1], B. Navayi Neya[2,*], J. Vaseghi Amiri[2]

Received: September 2013, Revised: November 2013, Accepted: December 2013

Abstract

This study focuses on non-linear seismic response of a concrete gravity dam subjected to translational and rotational correlated components of ground motions including dam-reservoir interaction. For this purpose rotational components of ground motion is generated using Hong Non Lee improved method based on corresponding available translational components. The 2D seismic behavior of the dam concrete is taken into account using nonlinear fracture mechanics based on the smeared- crack concepts and the dam-reservoir system are modeled using Lagrangian-Lagrangian approach in finite element method. Based on presented formulation, Pine Flat concrete gravity dam is analyzed for different cases and results show that the rotational component of ground motion can increase or decrease the maximum horizontal and vertical displacements of dam crest. These results are dependent on the frequency of dam-reservoir system and predominant frequencies of translational and rotational components of ground motion.

Keywords: *Rotational component of ground motion, Nonlinear analysis, Concrete gravity dam, Smeared crack, Dam-Reservoir interaction, Lagrangian-Lagrangian method.*

1. Introduction

To complete seismic evaluation of concrete dams using finite element method, some considerations are very important. The effect of fluid-structure interaction, nonlinear behavior of dam material and the earthquake loading are some of these considerations. In the dynamic analysis of concrete dams, the interaction effects of the impounded water can be represented by any of three basic approaches. The simplest one is the added mass attached to the dam [1]. Another approach describing the dam-water interaction is the Eulerian approach. In this approach, variables are displacements in the structure and pressures or velocity potential in the fluid. Since these variables in the fluid and structure are different in this approach, a special-purpose computer program for the solution of coupled systems is required [2,3]. The Lagrangian approach is a third way to represent the fluid-structure interaction. In this approach, behavior of fluid and structure are expressed in terms of displacements and some constrains and Penalty functions are suggested to eliminate the zero-energy modes [4, 5]. This approach is also used by many researchers to dynamic analysis of dams [6-9].

** Corresponding author: Navayi@nit.ac.ir*

1 Ph.D Candidate, Babol Noshirvani University of Technology, Babol, Iran

2 Associate Professor, Civil Engineering Department, Babol Noshirvani University of Technology, Babol, Iran

Seismic fracture analysis of concrete gravity dams has long been a topic of research in dam engineering for linear and nonlinear fracture mechanics. In regard to the application of nonlinear fracture mechanics to the cracking study of mass concrete, there are two basic procedures of modeling cracks commonly used in numerical analysis, namely the fictitious crack model (FCM) presented by Hillerborg et al. [10] and the crack band model (CBM) by Bazant et al. [11-13], both of which take the effects of strain softening into account by different assumptions. Many other researchers [14-19] is also have studied the seismic fracture of concrete gravity dams using several crack models, failure criteria, different fracture modes and constitutive behavior of concrete but any of these researches don't have the same result for the path of crack propagation with the observed prototype behavior.

The kinematics of any point in a medium is ideally expressed in terms of three translational and three rotational components. Newmark [20] was perhaps the first to establish a relationship between the torsional and translational components using classical elasticity theory based on constant wave velocity. This method was used by several authors [21-23]. Other researchers [24-27] have used elastic wave propagation theory in the soil medium together with the classical elasticity theory. During the past decades, in spite of the fact that numerous studies have continued to show the significance of the rotational components in strong motion excitation on the structural response, the progress in developing and deploying strong motion instruments capable of recording the rotational

components of earthquake waves has continued to be slow [28-30].

Generally, in seismic analysis of concrete dams and other structures, it is assumed that the system is subjected to translational components of ground motion and the rotational components of ground motion are implicitly assumed to be insignificant. Recently it has been shown that the rotational components of ground motion can be noticeable effects on the dynamic response of structures and many structural failures and the damage caused by earthquakes can be linked to mentioned effects [31-38]. It has shown that during an earthquake, even symmetric structures can be expected to undergo substantial torsional excitation and in the case of stiff building structures, the torsional components can increase the displacements up to four times [35]. However these effects on the nonlinear dynamic response of concrete gravity dams are not considered in previous researches.

In this paper, a numerical scheme based on the crack band theory is presented to study the nonlinear fracture behavior of concrete gravity dams under translational and corresponding rotational components of ground motion due to earthquakes. The foundation is assumed to be rigid and its interaction with dam and reservoir are not taken in to account. The fluid is also assumed to be isotropic, inviscid and irrotational. First, the rotational components of six earthquakes are obtained using translational available components based on Hong Non Lee method [26] and then the nonlinear response and cracking path of Pine Flat concrete gravity dam are compared with and without considering the rotational components.

2. Lagrangian Formulation of Fluid-Structure Interaction System

In this paper considering linear-elastic, inviscid, and irrotational fluid, the equations of motion of the dam-reservoir system are determined using the Lagrangian approach. For a two-dimensional fluid element, the stress-strain relationships can be written as:

$$\begin{Bmatrix} P \\ P_w \end{Bmatrix} = \begin{bmatrix} C_{11} & 0 \\ 0 & C_{22} \end{bmatrix} \begin{Bmatrix} \varepsilon_v \\ w \end{Bmatrix} \tag{1}$$

where P, C_{11} and ε_v are pressures, bulk modulus and volumetric strains of the fluid, respectively. The rotation and constraint parameters are included in the stress–strain equation of the fluid, since the irrotationality of the fluid is considered by penalty function methods [4,5]. In Eq. (1), w is the rotation about the axis normal to the plane, P_w is the rotational stress and C_{22} is the constraint parameter [5, 39].

The equations of motion for a system can be derived directly from Lagrange's equations. These equations are a direct result of Hamilton's variation principle under the specific condition that the energy and work terms can be expressed in terms of the generalized coordinates and of their time derivatives and variations [39].

Based on Lagrangian approach, the equation of motion can be presented as:

$$M_f \ddot{U}_f + C_f \dot{U}_f + K_f^* U_f = R_f \tag{2}$$

in which C_f, K_f^*, $\ddot{U}_f$ and $\dot{U}_f$ are the fluid damping matrix, stiffness matrix including the free surface stiffness, the nodal acceleration and displacement vectors of finite element mesh, respectively. R_f is a time-varying nodal force vector defined as $M_f a_g$ when the earthquake ground acceleration is applied to the fluid system in which a_g is ground acceleration vector. In the formation of the fluid element matrices in Lagrangian approach, reduced integration orders were utilized to decrease the fluid element stiffness.

The equations of motion of the fluid system, Eq. (2), have a similar form to those of the structure system. To obtain the coupled equations of the fluid-structure system, a determination of the interface condition is required. Because of the fluid is assumed to be inviscid, only displacement in normal direction to the interface is continuous at the interface of the system. This assumption has been not caused any observed approximation in dam response [39].

Assuming that positive face is the structure and negative face is the fluid, the boundary condition at the fluid-structure interface is

$$U_n^- = U_n^+ \tag{3}$$

where U_n is the normal component of the interface displacement [18]. This equation is satisfied using the interface elements with stiffness matrix K_{int}.

Using the mentioned equations, the equations of motion of the coupled system subjected to ground motion including damping effects are given by:

$$M_c \ddot{U}_c + C_c \dot{U}_c + K_c U_c = R_c \tag{4}$$

in which M_c, C_c and K_c are the mass, damping and stiffness matrices for the coupled system. U_c, $\dot{U}_c$ and $\ddot{U}_c$ are the vectors of the displacement, velocity, acceleration of the coupled system and R_c is the time-varying nodal forces vector of ground acceleration.

In this research, the governing equation for dam-reservoir system is solved by Bosak method and for nonlinear analysis, the displacements and forces at joints of finite element mesh are selected for convergence criteria in Newton-Raphson scheme.

3. Numerical Model for Fracture Analysis of Mass Concrete

In smeared crack models, the fracture process is initiated when the maximum principal stress in a material point exceeds its tensile strength. In the crack band theory, when an opening cracks (Mode I) initiates, the fracture process of mass concrete can be depicted by progressive micro-cracking of the material in a crack band. The crack propagation is mainly controlled by the shape of the tensile-softening diagram and the energy absorbed in the crack band of the softening zone per unit cross-section area is defined as the fracture energy G_f , which is a characteristic parameter of the material.

In this research the orthogonal multi fixed smeared crack are used to study the 2D seismic fracture behavior of concrete gravity dams considering opening and shearing modes of crack (Mode I and II). For this purpose four steps are considered in calculations including: crack initiation criterion or pre-cracking, the post cracking behavior, crack modeling and the closing and reopening of crack.

The pre-cracking behavior of concrete is assumed to be linear and elastic. To consider the nonlinearity of concrete behavior in elastic cases as shown in Fig.(1-a) and also the effect of two axial stresses, the crack initiation criterion using the tensile strain energy can be written as [14]:

$$\frac{\sigma_1}{\sigma_i} = \left(\frac{\sigma_1}{\sigma_1 - \nu\sigma_2}\right)^{\frac{1}{2}} \tag{5}$$

This equation can be shown as Fig. (1-b) where σ_1 and σ_2 are the principle stresses in an element, $\sigma_i = 1.3 f_t$ in which f_t is the uniaxial tensile strength of the concrete [14] and ν is the poison ratio. Thus herein, when the maximum average principal stresses in Guess pints of an element exceeds the Eqs. (5), the first crack is assumed to form in the element perpendicular to the maximum principle stress according to Fig. (2).

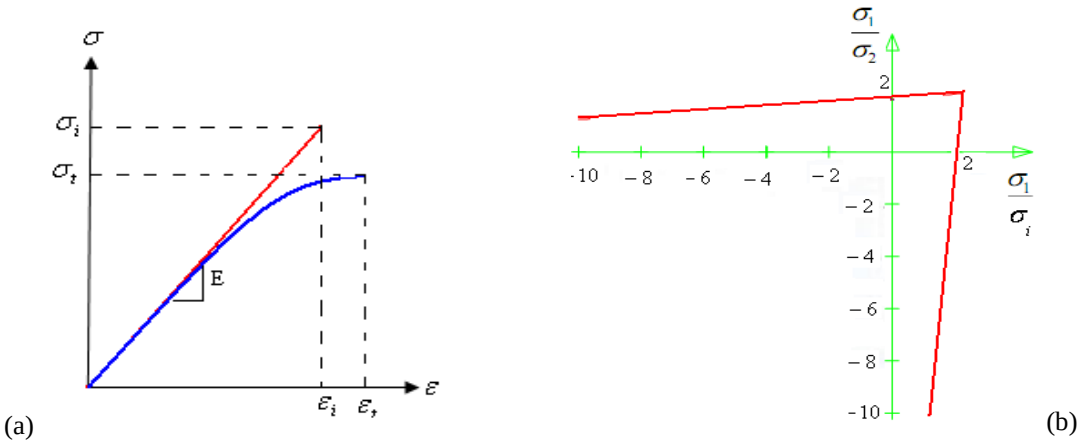

(a) (b)

Fig. 1 (a) nonlinear elastic behavior of concrete, (b) Crack initiation criterion [14]

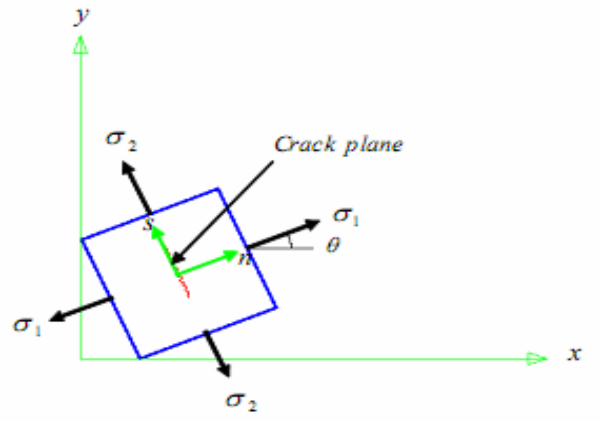

Fig. 2 Crack element and local coordinates

After crack initiation the concrete behaves as a strain-softening material, for which the tensile stress normal to the crack decreases with increasing strain. The specific softening constitutive relation can be obtained from uniaxial tensile tests of a concrete specimen with deformation control. For the complete stress-strain relation as shown in Fig. 3, E , E_s and E_t are the initial modulus, the current secant modulus and the tangential modulus, respectively. e_n is the total strain in local coordinates

which is decomposed in two strains, the crack and the concrete strains(e^{cr}, e^{co}). The fracture energy G_f can be evaluated from [13]:

$$G_f = h_c \int S_n^{cr} de_n \tag{6}$$

where h_c represents the crack band width of the fracture process zone given by the characteristic length of the material; for concrete it is suggested [18] that $h_c = 3d$ with $\boldsymbol{d}$ denoting the maximum aggregate size in the concrete.

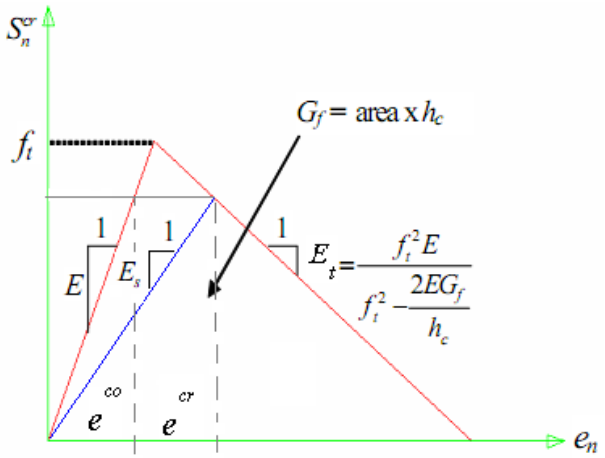

Fig. 3 Complete stress-strain curve in tension [18]

In finite element analysis, when the size of the element which models the width of the crack band is greater than h_c, the softening constitutive curve needs to be modified according to Bezant's energy criterion [13] so that the fracture energy remains the same. Thus, the results remain independent of the element size.

As shown in Fig. (4-a), in dynamic case analyses, the initial modulus and the tensile strength are increased using the coefficients 1.25 and 1.5, respectively [14]. The shape of softening curve also can be changed in the form of multi-linear as shown in Fig. (4-b), to consider size effect of structure and more realistic model to match the experimental results [18].

In Fig. (4):

$$D_{i,bl}^{I} = \frac{\alpha_2 + (1-\alpha_2)\alpha_1^2}{\alpha_2}\left(-\frac{f_t^2 h_c}{2G_f}\right) = \frac{\alpha_2 + (1-\alpha_2)\alpha_1^2}{\alpha_2} D_{i,l}^{I} \tag{7}$$

where α_1 and α_2 is obtained using the experimental results[17]. If the $\alpha_1 = 0$ or the $\alpha_2 = 1$, then $D_{i,bl}^{I} = D_{i,l}^{I}$ and the linear softening behavior is resulted.

The total stress-strain relation for a concrete element undergoing cracking is given by:

$$\left\{S_n^{cr} \quad S_s^{cr} \quad \tau_{ns}\right\}^T = [D]_{ns} \left\{e_n \quad e_s \quad \gamma_{ns}\right\}^T \tag{8}$$

where subscripts n and s represent the local coordinates in according with the crack directions shown in Fig.(2) and $[D]_{ns}$ represents the material property matrix for the same local coordinate orientation and is given by [18]:

$$[D]_{ns} = \begin{bmatrix} D_{11} & D_{12} & 0 \\ D_{21} & D_{22} & 0 \\ 0 & 0 & D_{13} \end{bmatrix} \tag{9}$$

where:

$$D_{11} = \frac{\eta_1 E}{1-\nu^2\eta_1\eta_2}, D_{22} = \frac{\eta_2 E}{1-\nu^2\eta_1\eta_2}, D_{12} = D_{21} = \frac{\nu\eta_1\eta_2}{1-\nu^2\eta_1\eta_2}, D_{33} = \overline{\beta}G$$
$$\overline{\beta} = \frac{\beta_1\beta_2}{(1-\beta_1)\beta_2 + \beta_1} \tag{10}$$

In Eqn.(9), $\eta_1 = \frac{E_{sn}}{E}$ and $\eta_2 = \frac{E_{ss}}{E}$ are the ratio between secant and initial modulus in n and s directions, respectively. β_1 and β_2 are also the shear retention factor representing the extent of aggregate interlock on the crack surfaces and for multi fixed crack model are obtained using [18]:

$$\beta_1 = \beta_{\max}\left(1 - \frac{e_n^{cr1}}{e_n^{f}}\right)$$
$$\beta_2 = \beta_{\max}\left(1 - \frac{e_n^{cr2}}{e_n^{f}}\right) \tag{11}$$

where e_n^{f} is the total crack strain, $\beta_{\max}$ is the maximum shear retention factor for the cracked element and e_n^{cr1}, e_n^{cr2} are the crack strains for crack number 1 and 2, respectively.

The stress-strain matrix $[D]_{ns}$ is transferred to Cartesian coordinates using [18]:

$$[D]_{xy} = [T]^T [D]_{ns} [T] \tag{12}$$

During the process of cyclic loading, the cracks may close and reopen both periodically and progressively. Based on the results of cyclic tensile tests given in Ref. [17], the simplified constitutive model accounting for crack closing and reopening shown in Fig. (5) is adopted. The element remains linear with modulus of E before cracking and also subsequently after the crack closes. Whenever the stress normal to the crack surface becomes positive (tensile) again, the crack will reopen with continuously decreasing secant modulus E_s until a macro-crack forms at strain $e_n = e_n^{f}$.

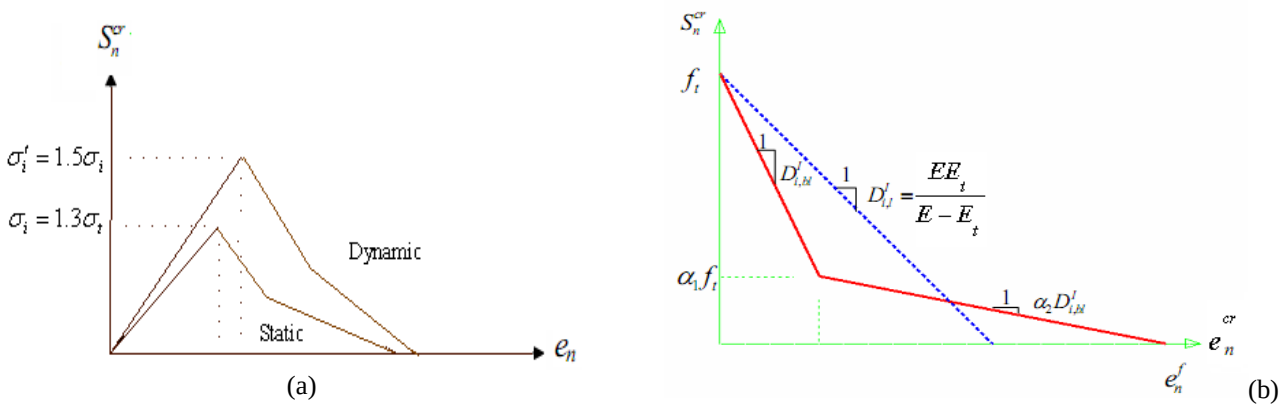

Fig. 4 (a) static and dynamic softening curve [14], (b) the stress-strain multi-linear behavior after cracking [18]

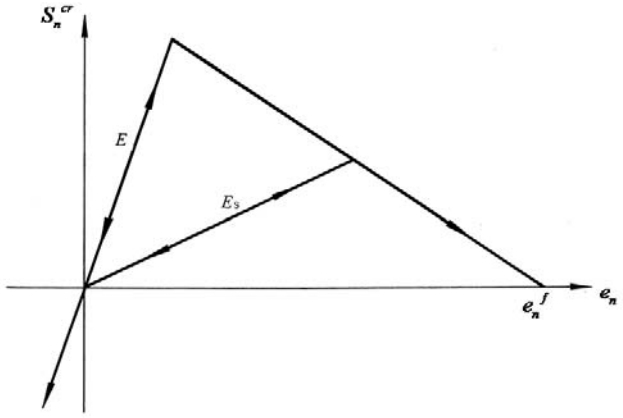

Fig. 5 Closing- reopening behavior of concrete material [16,17]

4. Rocking Component of Ground Motion

Ideally, the kinematics of any point in the medium is three translational and three rotational components where the three rotational components of ground motion include the two rocking components and one torsional component. The three translational components are easily measurable by standard techniques, whereas the rotational components are not directly accessible. In this research the rocking component of earthquake ground motion are generated using classical elasticity and elastic wave propagation theories considering frequency dependent wave velocities. Then these correlated components are applied properly to the finite element mesh of concrete gravity dam.

4.1. Generation the rocking component of ground motion

In order to 2D seismic analysis of gravity dams, two translational components of ground motion in x and z directions and their related rocking component are used. These motion components are shown in Fig. (6) by symbols u , w and ϕ_{gy}. In addition for SV wave incidence, the amplitudes of incident wave and reflected P and SV. waves are shown in this figure by A_S, A_{SP} and A_{SS} and their angles with vertical axes are shown by θ_0, θ_1, θ_2 respectively.

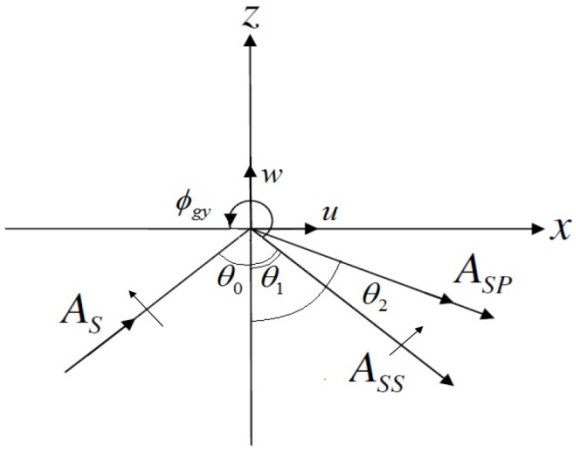

Fig. 6 Propagation of SV wave on the ground surface

The rocking component using classical elasticity theory can be written as [24]:

$$\phi_{gy} = \frac{1}{2}\left(\frac{\partial w}{\partial x} - \frac{\partial u}{\partial z}\right) \tag{13}$$

Using elastic wave propagation theory and the potential functions of wave motion with frequency ω and by imposing the free shear stress condition at the ground surface, the Eqs.(13) can be rewritten as [36-38]:

$$\varphi_{gy} = \frac{i\omega}{C_x} w = (1e^{\frac{\pi}{2}i})(\frac{\omega}{C_x})(R_w.e^{i\theta_w}) = (\frac{\omega}{C_x} R_w)(e^{(\frac{\pi}{2}+\theta_w)i}) \quad (14)$$

where $C_x = \beta / \sin\theta_0$ is the frequency dependent wave velocity and β is the propagation velocity of shear wave.

Eqs. (14) show that the rocking component has the amplitude equal to $\frac{\omega}{C_x} R_w$ where R_w is the amplitude of vertical component of ground motion. In addition the phase difference between rocking and vertical ground motion is $\pi/2$.

Using improved approach developed by [26], by introducing $(x = \sin\theta_0)$ and based on Snell's law, Eqs. (15) and (16) are used to obtain the angle of incident wave.

$$G = \frac{2x\sqrt{1-K^2x^2}}{K(1-2x^2)},\ \theta_0 \prec \theta_C \quad (15)$$

$$G = -\frac{2x\sqrt{1-K^2x^2}}{iK(1-2x^2)},\ \theta_0 \succ \theta_C \quad (16)$$

where $G = w/u$ for rocking component in *x-z* plane due to SV wave; $K = \alpha/\beta$ and $\theta_C = \arcsin(\beta/\alpha)$ is the incident critical angle. α is the propagation velocity of P wave.

Fig. 7 illustrates the flowchart of calculation the rotational components of ground motion using translation components.

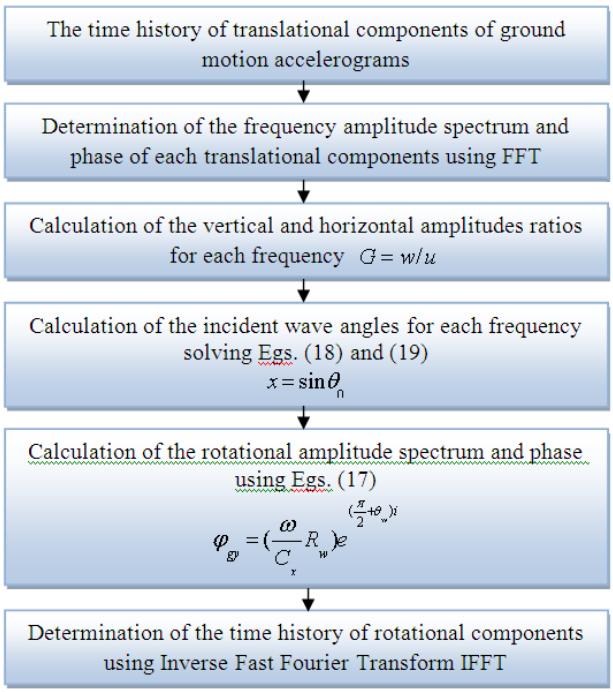

Fig. 7 Flowchart for calculation of rotational components of ground motion

4.2. Applied force due to ground rotation

In Eqs. (4), to obtain the nodal forces vector due to translational and rotational ground acceleration, R_c, the rigid body kinematics theory [41] is used. In this theory the general motion of rigid body can be divided into two translational and rotational motions as shown in Fig. (8).

In this case:

$$R_c = M_c \left\{\ddot{U}_g(t)\right\} \quad (17)$$

where:

$$\left\{\ddot{U}_g(t)\right\} = \begin{Bmatrix} \ddot{u}_g(t) + \ddot{\phi}_{gy}(t) z - \dot{\phi}_{gy}(t)^2 x \\ \ddot{w}_g(t) - (\ddot{\phi}_{gy}(t) x + \dot{\phi}_{gy}(t)^2 z) \end{Bmatrix} \quad (18)$$

in Eqs.(4) $\ddot{u}_g(t)$ and $\ddot{w}_g(t)$ are the time-varying of translational acceleration, $\ddot{\phi}_{gy}(t)$ and $\dot{\phi}_{gy}(t)$ are the time-varying of rotational acceleration and velocity respectively and x, z are coordinates of each nodes [25].

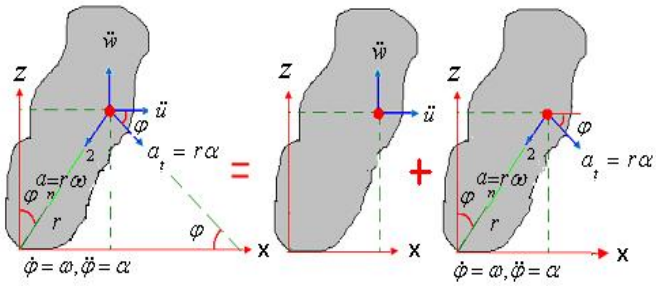

Fig. 8 The general motion of rigid body

5. Numerical Result

Based on proposed formulation for calculation of dam-reservoir response under rotational and translational components of ground motion, a computer code have been prepared in Fortran 91 by authors.

For this purpose the tallest monolith of the Pine Flat Dam is selected for evaluation of the results Geometrical characteristics and finite element model of Pine Flat dam-reservoir system are shown in Fig. 9 in which maximum water level is 116.2 m and the reservoir's length is considered three times as long as the water level and the Somerfield boundary condition is used for radiation condition in truncated far end of reservoir [8,42].

The material properties adopted in the analysis are shown in Table 1 [14,15]. In this table the Bulk constant, K, is related to elasticity modulus, E, using $K = \frac{E}{3(1-2\nu)}$ for same materials Stiffness proportional damping is assumed with the damping coefficient calibrated to provide $\zeta = 0.05$ for the fundamental mode

of the initial linear structure and $\zeta = 0.01$ for the reservoir [7]. The bilinear softening curve of Ahmadi [14] has been employed to verify the nonlinear response of dam-reservoir system. Then multi-linear softening curve of [18] has been used to obtain other results. For multi-linear softening curve, the shape of curve are defined using $\alpha_1 = 0.3$, $\alpha_2 = 0.2$ [18].

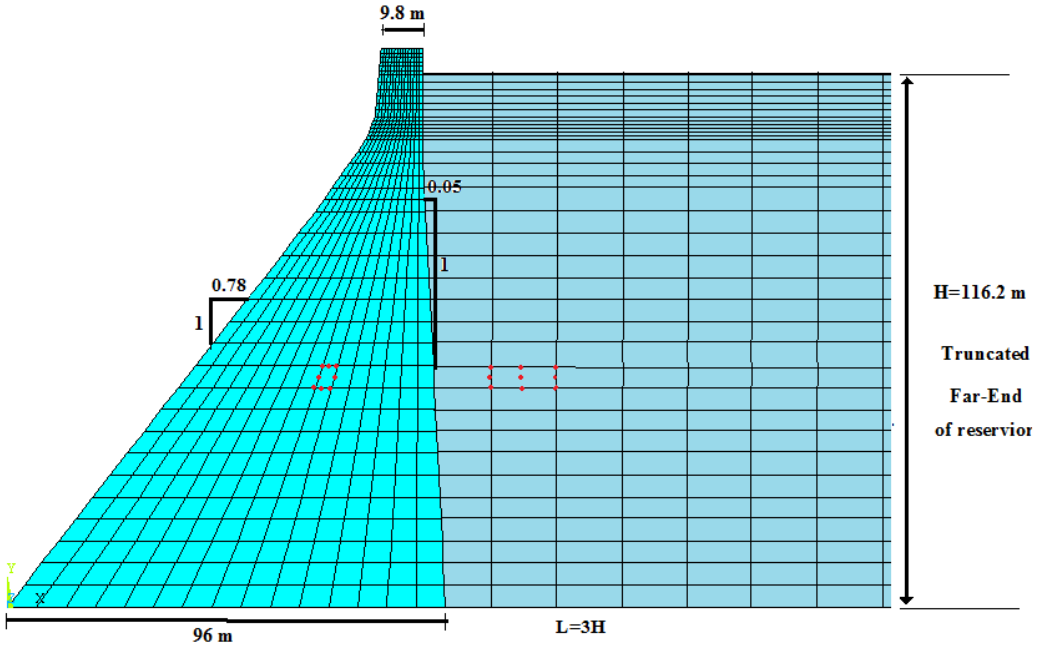

Fig. 9 Dimensions of the tallest monolith of Pine Flat dam and it finite element mesh

Table 1 Material properties of Pine Flat dam

Material	Bulk Constant *K(MPa)*	Tensile strength f_t *(MPa)*	Poisson's ratio	Damping ratio	Fracture energy *G (N/m)*	Unit Weight $\gamma(kN/m^3)$
Concrete	15556	2.93	0.2	0.05	150	24.5
Water	2000	-	-	0.01	-	10

In this paper translational components of six earthquakes are used to generate their corresponding rotational components. Characteristics of translational components of these earthquakes and their rotational components where are obtained using mentioned equations in part 4 are presented in Tables 2 and 3, respectively. The rotational Fourier amplitude spectrums are also shown in Fig. 10.

Table 2 Characteristics of earthquakes

Earthquake (Date)	Station	Magnitude (Rishter)	Epicentral Distance(km)	Field	Component	PGA (g)	Shear Velocity
Imperial Valley (1951/01/24)	117 El Centro	5.60	28.24	far	Up-Down North-South	0.013 0.029	213.4
San Fernando (1971/02/09)	Pacoma Dam	6.61	11.86	near	Vertical S74W	0.709 1.075	2016.1
Taft (1952/7/21)	Lincoln School	7.36	35	far	Vertical S69E	0.155 0.179	385.4
Tabas, Iran (1978/09/16)	Boshrooyeh	7.35	74.66	far	Vertical Longitudinal	0.069 0.109	338.6
Chi Chi Taiwan (1999/09/20)	CWB99999 17ALS	7.62	37.83	far	Vertical North-South	0.074 0.175	553.4
Northridge (1994/01/17)	000LA Dam	6.69	11.79	near	Vertical Longitudinal	0.424 0.511	629.1

Table 3 Characteristics of rotational components for six earthquakes ground motion.

Earthquake	$\ddot{\varphi}_{max}(mrad/s^2)$	$\dot{\varphi}_{max}(mrad/s)$	Predominate Frequency *(Hz)*		
			Horizontal Comp.	Vertical Comp.	Rocking Comp.
Imperial Valley	-6.17	-0.030	2.25	4.45	1.65
San Fernando	-57.00	0.370	4.78	4.25	11.20
Taft	15.60	-0.043	4.40	2.30	1.30
Tabas, Iran	-108.50	0.376	7.40	0.90	0.88
Chi Chi Taiwan	11.50	0.054	0.70	0.75	0.75
Northridge	447.40	-1.220	0.78	10.25	1.10

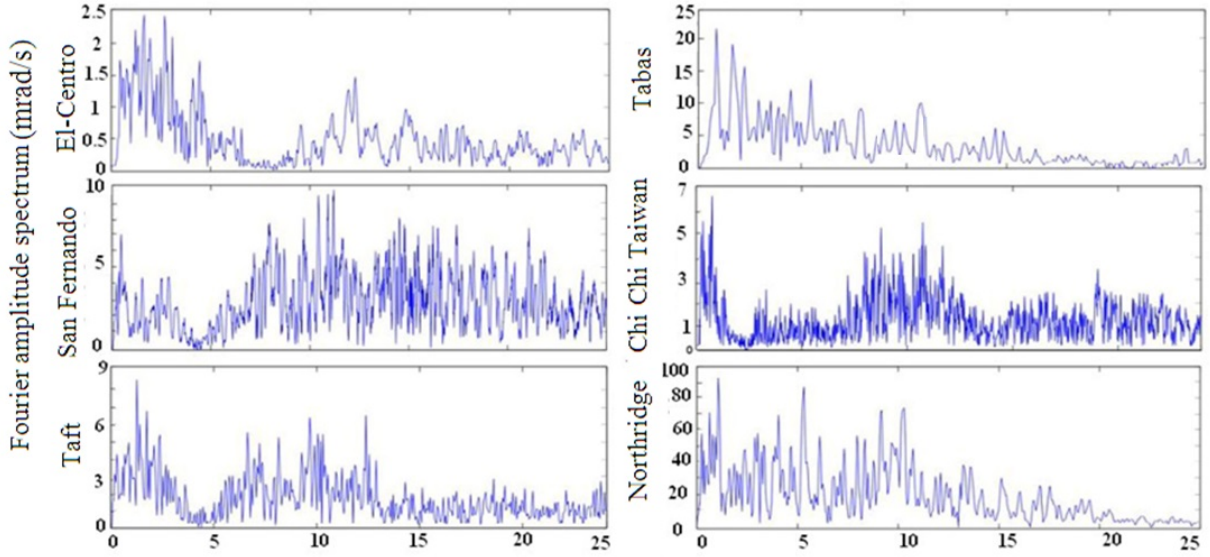

Fig. 10 Rocking Fourier amplitude spectrums for six earthquakes

5.1. Verification

To evaluate the Hong Non Lee improved method, the rotational components of the San Fernando earthquake is obtained using Hong Non Lee improved method [26]. Using this method, it is found that the peak values of rocking and torsional accelerations for shear wave velocity of 300 m/s are 0.3833 rad/s^2, -0.2545 rad/s^2, respectively. These values are calculated in [27] equal to -0.3725 rad/s^2, -0.2480 rad/s^2, respectively where the differences between these results are less than 3 percent. This difference is due to different ratio of ω / C_x where is considered constant in [27] and frequency dependent in this research. The time histories of rocking component for San Fernando earthquake which are generated by [27] and present work are shown in Fig. 11.

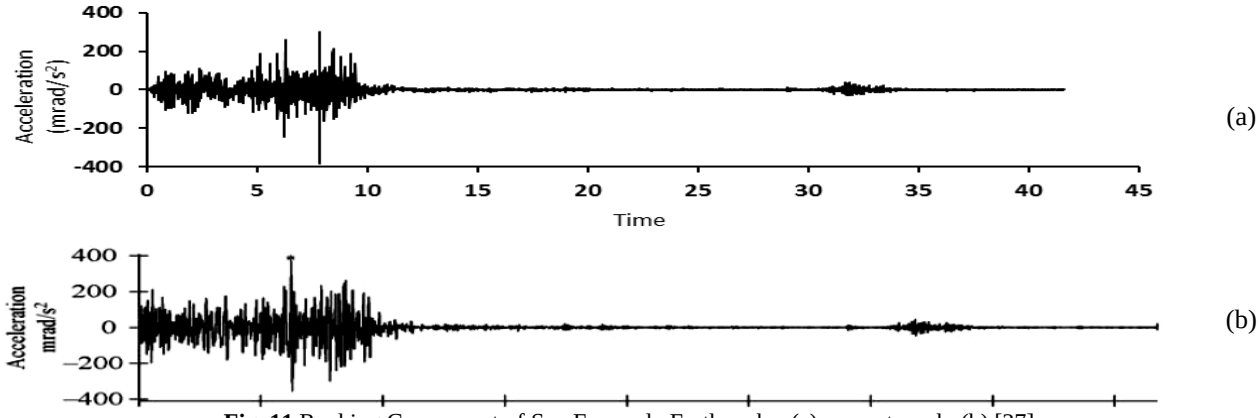

Fig. 11 Rocking Component of San Fernando Earthquake, (a) present work, (b) [27]

To evaluate the seismic response of dam-reservoir system under translational components of ground motion and study the finite element formulation for dynamic analysis of concrete gravity dam, some finite element analysis of system are done and the results are compared with analytical results or others works. For example the linear response of Pine Flat dam due to S69E component of Taft earthquake which is obtained in present work is

compared with result by [42]. These results are shown in Fig. 12 which have very good agreements.

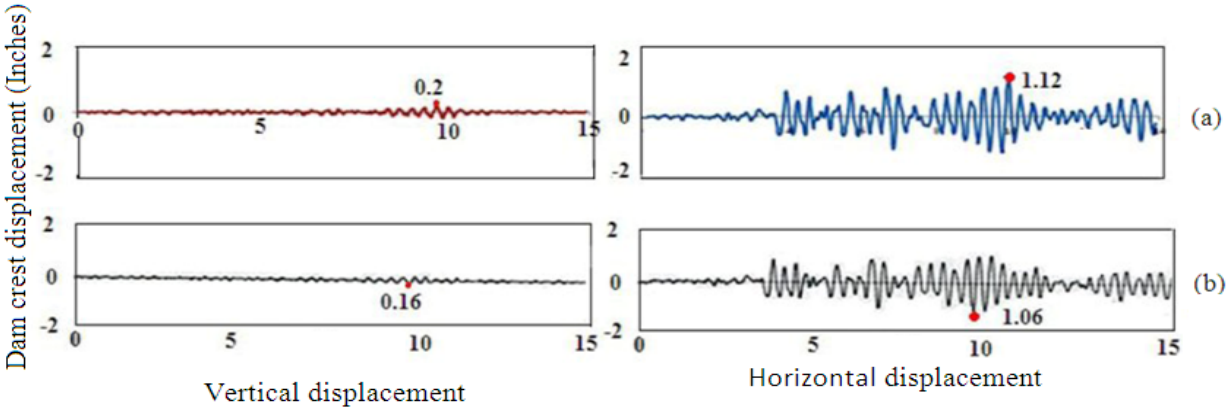

Fig. 12 The linear response of Pine Flat dam crest without reservoir due to S69E component of Taft earthquake, (a): present work, (b):[40,42]

5.2. Modal analysis

To study the behavior of dam subjected to translational and rotational components of earthquake, the modal analyses of dam-reservoir system with three levels of water have been done and the natural frequencies for two modes of them are listed in Table 4.

Table 4 The natural frequencies of dam-reservoir system (*Hz*)

System	Dam	Dam & 1/3 Full res.	Dam & 2/3 Full res.	Dam & Full res.
Mode 1	3.189	2.812	2.611	2.538
Mode 2	6.630	3.906	3.512	3.226
Mode 3	8.813	5.625	4.335	3.387
Mode 4	11.591	6.634	4.459	4.082
Mode 5	18.138	8.532	4.749	4.529

5.3. Seismic fracture analysis of pine flat dam

In this paper the fracture analysis of Pine Flat dam under the translational and rotational components of six earthquakes is conducted employing the numerical model described above. The time step used in the analysis is 0.0025 s is employed to solve the equation of motion. The responses of dam due to two translational components named "2C" and due to two translational components and their rotational correlated component named "2C+R" are analyzed and the normalized response of dam is calculated using the ratio between maximum response of dam due to (2C+R) and (2C).

Fig. 13 to 16 show the linear and nonlinear response of Pine Flat dam crest subjected to (2C) and (2C+R) of Taft earthquake.

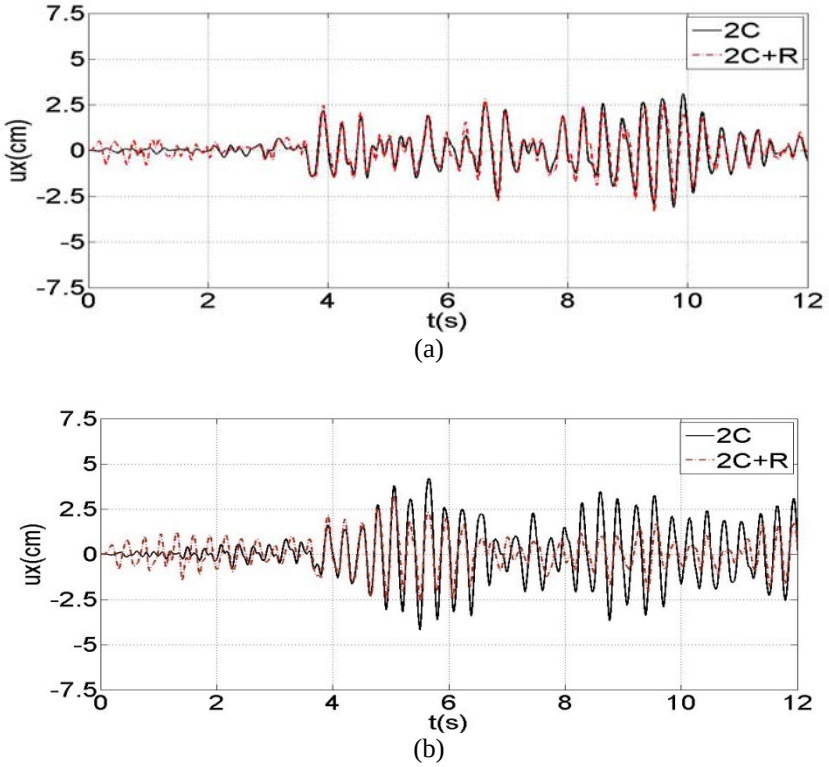

Fig. 13 The response of Pine Flat dam without reservoir due to (2C.) and (2C+R) of Taft earthquake, a) Linear response, b) Nonlinear

response

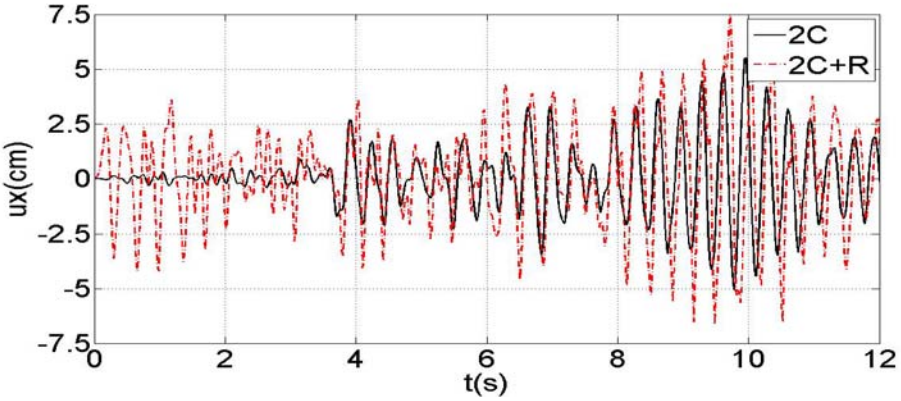

(a)

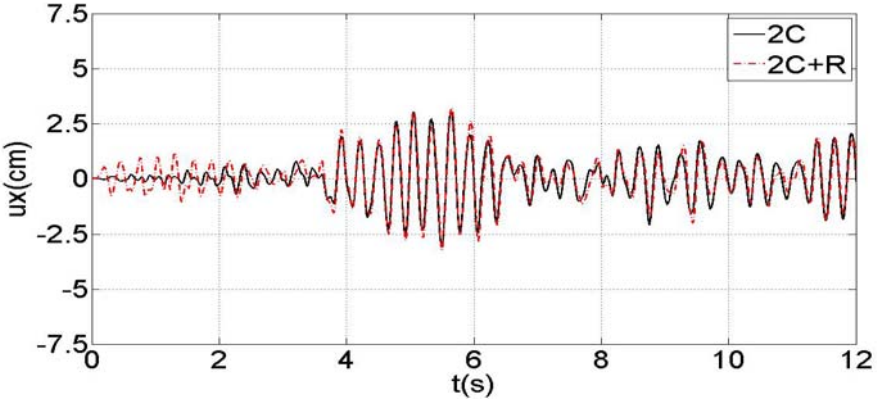

(b)

Fig. 14 The response of Pine Flat dam with 1/3 full reservoir due to (2C.) and (2C+R) of Taft earthquake, a) Linear response, b) Nonlinear response

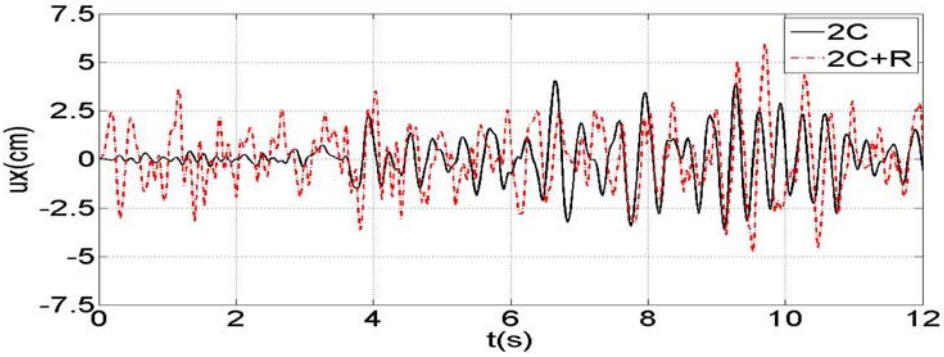

(a)

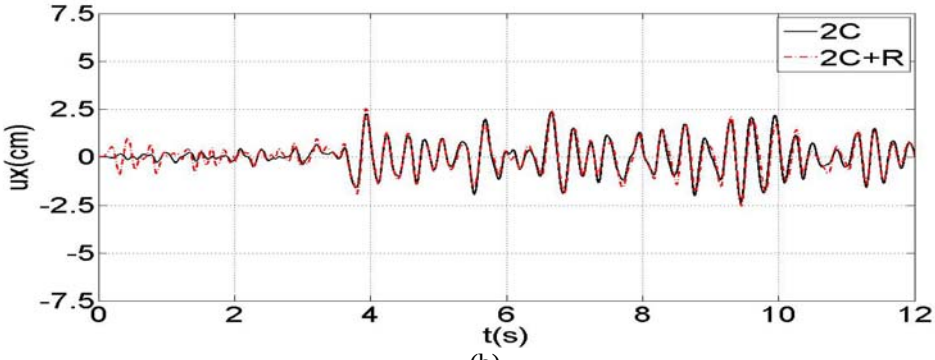

(b)

Fig. 15 The response of Pine Flat dam with 2/3 full reservoir due to (2C.) and (2C+R) of Taft earthquake, a) Linear response, b) Nonlinear response

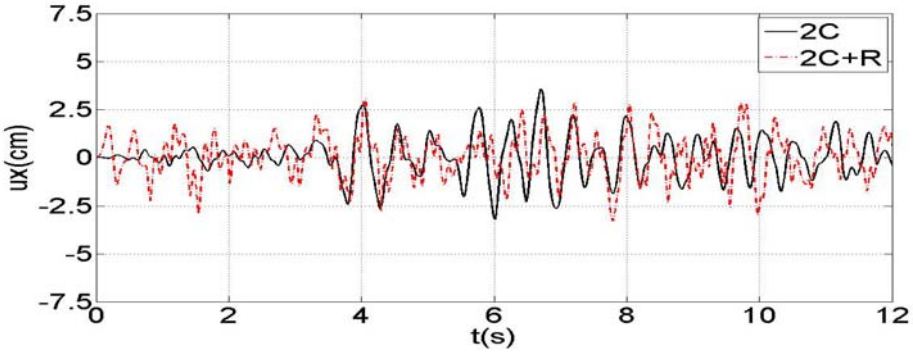

(a)

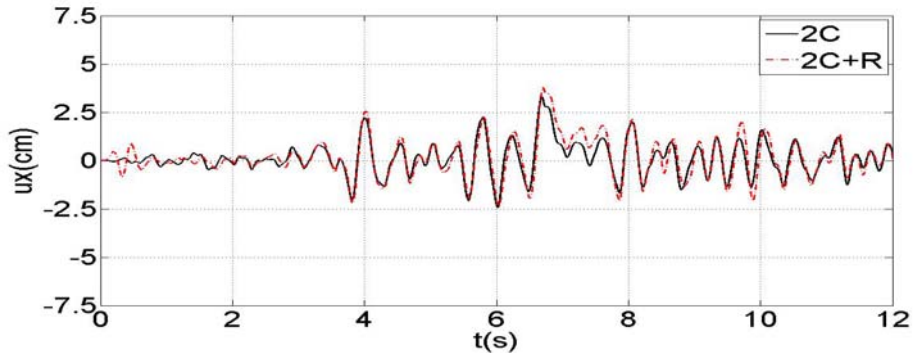

(b)

Fig. 16 The response of Pine Flat dam with full reservoir due to (2C.) and (2C+R) of Taft earthquake, a) Linear response, b) Nonlinear response

Fig. 17 also shows the nonlinear response of empty dam subjected to Chi Chi Taiwan earthquake . As shown in this figure, responses to (2C) and (2C+R) excitations are very close. Other nonlinear results such as maximum horizontal and vertical displacements subjected to (2C) and (2C+R) and their normalized response for six mentioned earthquakes are presented in Table 5.

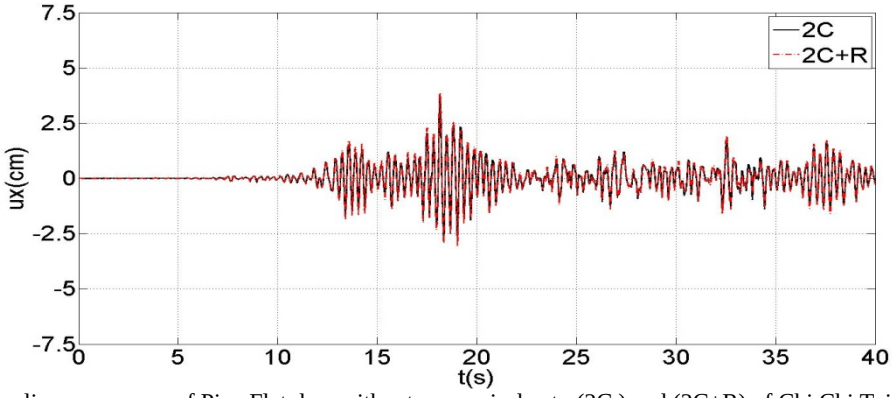

Fig. 17 The nonlinear response of Pine Flat dam without reservoir due to (2C.) and (2C+R) of Chi Chi Taiwan earthquake

Table 5 Nonlinear response of Pine Flat dam crest due to (2 Comp.) and (3 Comp.) of Ground motions

System	Earthquake	Maximum Horizontal displacement(cm)		Normalized Horizontal displacement	Maximum Vertical displacement(cm)		Normalized Vertical displacement
		2C	2C+R		2C	2C+R	
Dam	Imperial Valley	0.729	1.444	1.981	0.213	0.427	2.005
	San Fernando	14.855	12.384	0.832	4.989	3.626	0.727
	Taft	4.201	3.197	0.761	1.222	0.755	0.617
	Tabas, Iran	0.787	5.805	7.371	0.329	1.526	4.628

Dam + 1/3full Reservior	Chi Chi Taiwan	2.214	2.247	1.015	0.662	0.719	1.086
	Northridge	4.284	16.855	3.934	8.113	5.965	0.735
	Imperial Valley	0.558	1.011	1.813	0.167	0.272	1.627
	San Fernando	15.970	18.650	1.168	5.140	5.180	1.008
	Taft	3.037	3.323	1.061	0.850	0.890	1.047
	Tabas, Iran	0.747	7.046	9.430	0.319	1.630	5.105
Dam + 2/3full Reservior	Chi Chi Taiwan	2.517	2.380	0.945	0.737	0.723	0.981
	Northridge	5.514	5.976	1.084	1.967	2.422	1.231
	Imperial Valley	0.507	0.551	1.085	0.151	0.148	0.982
	San Fernando	Failed at t=3.472	5.720	-	Failed at t=3.472	2.350	-
	Taft	2.300	2.500	1.088	0.720	0.740	1.023
	Tabas, Iran	0.903	6.840	7.575	0.351	1.310	3.732
Dam + Full Reservior	Chi Chi Taiwan	2.992	3.104	1.037	0.697	0.746	1.070
	Northridge	25.800	25.990	1.007	6.270	6.550	1.044
	Imperial Valley	0.607	0.785	1.294	0.187	0.205	1.095
	San Fernando	3.161	3.455	1.093	2.304	2.939	1.276
	Taft	3.940	4.950	1.257	2.070	2.260	1.091
	Tabas, Iran	0.711	8.528	11.990	0.355	12.200	34.390
	Chi Chi Taiwan	3.092	3.145	1.017	0.805	0.931	1.155
	Northridge	18.890	20.616	1.091	2.308	7.779	3.370

As shown in Figs. 13-17, the rotational component of ground motion can change both the quality and quantity of dam response and the maximum response of dam can increase or decrease when the rotational components of ground motion is considered. This effect is dependent on the natural frequency of dam and predominate frequency of rocking component. In addition, comparison of linear and nonlinear response of Pine Flat dam with different water level in reservoir are not same due to the post-cracking behavior of concrete material and changing of the material elasticity modulus after cracking.

As shown in Table 5, the maximum normalized response of horizontal and vertical displacements of dam crest for different level of water in reservoir under Tabas earthquake, while for minimum normalized response of displacements under other earthquakes there are not any regulation. In this table, the failure is occurred only due to translational components (2C) of San Fernando earthquake for dam with 2/3 full reservoir at time of t=3.472. In this case for (2C+R) analyses, when the rotational component is considered the failure will not occur and this phenomenon mean that the rotation component of ground motion decreases the response of dam. .

In Fig. 18, the crack propagation of dam without reservoir due to (2C) and (2C+R) of Taft earthquake are compared schematically. As shown in this figure, the rotational components change the cracking pattern and the crack zone in dam body is more limited, while for dam with full reservoir due to (2C) and (2C+R) under Tabas earthquake, the rotational component of ground motion increases the dam cracking zone (Fig. (19)).

(a)

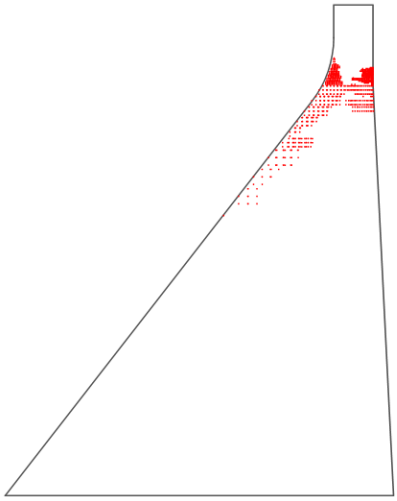

(b)

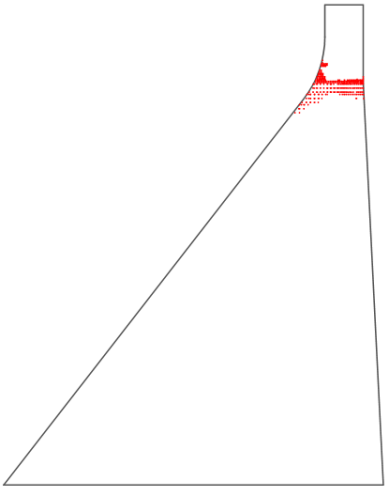

Fig.18 The Crack propagation of Pine Flat dam without reservoir subjected to Taft earthquake, (a): due to (2C), (b): due to (2C+R)

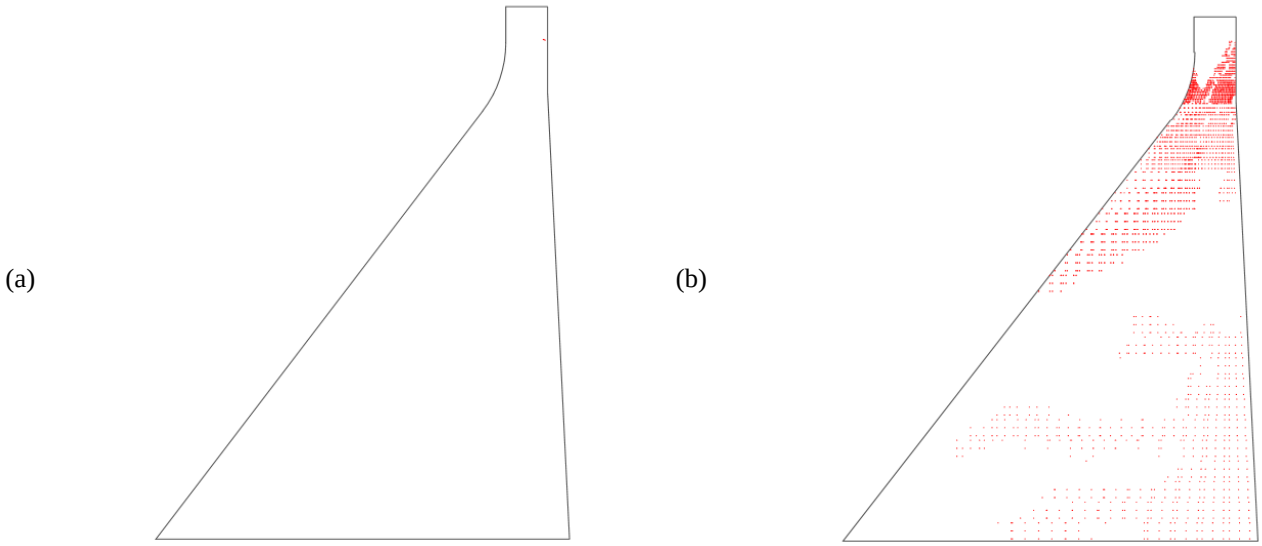

Fig.19 The Crack propagation of Pine Flat dam with full reservoir subjected to Taft earthquake, (a): due to (2C), (b): due to (2C+R)

6. Conclusions

In this study, nonlinear seismic response of a concrete gravity dam subjected to two translational components (2C) and two translational and their rotational correlated components (2C+R) are investigated. Pine Flat concrete gravity dam is chosen for analyses and dam-reservoir interaction is modeled using finite element method and Lagrangian-Lagrangian approach. Nonlinear behavior of dam concrete is idealized using nonlinear fracture mechanics based on smeared crack approach and the following conclusions are made:

1- The normalized response of dam is dependent on the peak rotational rate (PRR), frequency content of rotational components of ground motions, their power spectrum, and the natural frequency of dam-reservoir. Depend on the mentioned parameters, the rotation component of ground motion can increase or decrease the response of the dam. In this study the Northridge and Tabas earthquakes have a high PRR and also their rotational Fourier amplitude and power spectrum close to the dam natural frequency are higher than other earthquakes. Therefore these two earthquakes have more effects on the response of dam.

2- The rotational effects on dam response can be neglected when the Fourier amplitudes of translational components of ground motion close to the dam natural frequency are greater than rotational Fourier amplitude.

3- Depends on natural frequencies of dam-reservoir and rotational components of ground motion, the quality and quantity of dam response can be changed basically.

4- Rotation component of earthquakes can decrease or increase the cracked zone of concrete gravity dams depends on frequency content of ground motion and natural frequency of dam-reservoir system. In addition, the rotational component of earthquake can change the beginning point of crack in dam and consequently cracked zone.

5- The normalized response of dam crest in nonlinear analysis is different from those in linear ones. These differences in nonlinear analysis are due to the post-cracking behavior of concrete material and changing of the material elasticity modulus after cracking.

6- The effect of rotational components on dam response can be changed basically when the water elevation is higher in comparison with lower water elevations. In this case, the quality and quantity of dam response are also changed considerably.

The time histories of rocking components that are obtained in this study using improved approach have a good agreement with the other works.

References

[1] Westergard HM. Water pressure on dams during earthquakes, ASCE, 1933, pp. 418-433.

[2] Clough RW, Zienkiewicz OC. Finite element method in analysis and design of dams, International Symposium of Criteria and assumptions for numerical analysis of dams, 1975, Swansea.

[3] Hariri MA, Mirzabozorg H, Kianoush R. Comparative study of endurance time and time history methods in seismic analysis of high arch dams, International Journal of Civil Engineering (IJCE), 2013, No. 2, Vol. 12, pp. 219-236.

[4] Hamdi MA, Ousset Y, Verchery G. A displacement method for the analysis of vibration of coupled fluid-structure systems, International Journal for Numerical Methods in Engineering, 1978, Vol. 13, pp. 139-150.

[5] Wilson EL, Khalvati M. Finite elements for the dynamic analysis of fluid-solid systems, International Journal for Numerical Methods in Engineering, 1983, Vol. 19, pp. 1657-1668.

[6] El-Aidi B, Hall JF. Nonlinear earthquake response of concrete gravity dams, part. 1: Modeling, Earthquake Engineering & Structural Dynamics, 1989, Vol. 18, pp. 837-851.

[7] El-Aidi B, Hall JF. Nonlinear earthquake response of concrete gravity dams, part. 2: Behavior, Earthquake

Engineering & Structural Dynamics, 1989, Vol. 18, pp. 853-865.
[8] Navayi Neya B. Mathematical modeling of concrete gravity dams under earthquake loading considering construction joints, Ph.D Thesis, Moscow Power Engineering Institute, 1998.
[9] Greeves EJ. The modeling and analysis of linear and nonlinear fluid-structure systems with particular reference to concrete dams, Ph.D. Thesis, Department of Civil Engineering, University of Bristol, 1991.
[10] Hillerborg A, Modeer M, Petersson PE. Analysis of crack formation and crack growth in concrete by means of fracture mechanics and finite elements, Cement and Concrete Research, 1976, No. 6, Vol. 6, pp. 773-782.
[11] Bazant ZP, Oh BH. Crack band theory for fracture of concrete, Matériaux et Construction, 1983, No. 93, Vol. 16, pp. 155-177.
[12] Bazant ZP, Cedolin L. Blunt crack band propagation in finite element analysis, Journal of the Engineering Mechanics Division, ASCE, 1979, No. 2, Vol. 105, pp. 297-315.
[13] Bazant ZP. Mechanics of distributed crackings, ASME, Applied Mechanics Reviews, 1986, 39(5), 675-705.
[14] Ahmadi MT, Vaseghi Amiri J. A new constitute model for nonlinear fracture analysis of concrete gravity dams including earthquake, International Journal of Engineering Science, 1998, No. 3, Vol. 9, pp. 23-42. (In Persian).
[15] Ghaemian M, Ghobarah A. Nonlinear seismic response of concrete gravity dams with dam-reservoir interaction, Engineering Structures, 1999, Vol. 21, pp. 306-315.
[16] Wang Guangluna OA Pekaub, Zhang Chuhana, Wang Shaomin. Seismic fracture analysis of concrete gravity dams based on nonlinear fracture mechanics, Engineering Fracture Mechanics, 2000, Vol. 65, pp. 67-87.
[17] José Sena Cruz, Joaquim Barros, Álvaro Azevedo. Elasto-plastic multi-fixed smeared crack model for concrete, Report 04-DEC/E-05, 2006.
[18] Cai Q. Finite element modeling of cracking in concrete gravity dams, Ph.D Thesis in Univercity of Pretoria, 2007.
[19] Attarnejad A, Kalateh F. Numerical simulation of acoustic cavitation in the reservoir and effects on dynamic response of concrete dams, International Journal of Civil Engineering (IJCE), 2012, No. 1, Vol. 10, pp. 72-86.
[20] Newmark NM. Torsion in symmetrical buildings, In: Proceeding of the 4th World Conference on Earthquake Engineering, 2, Santiago, Chile, 1969, A3.19-A3.32.
[21] Ghafory-Ashtiany M, Singh MP. Structural response for six correlated earthquake components, Earthquake Engineering & Structural Dynamics, 1986, Vol. 14, pp. 103-119.
[22] Huang BS. Ground rotational motions of the 1999 Chi Chi, Taiwan earthquake as inferred from dense array observations, Geophysical Research Letters, 2003, Vol. 30, pp. 1307-1310.
[23] Spudich P, Steck LK, Hellweg M, Fletcher JB, Baker LM. transient stresses at parkfield, California, produced by the M7.4 landers earthquake of june 28, 1992, observation from the UPSAR dense seismograph array, Journal of Geophysical Research, 1995, Vol. 100, pp. 675-690.
[24] Trifunac MD. A note on rotational components of earthquake motions on ground surface for incident body waves, International Journal of Soil Dynamics and Earthquake Engineering, 1982, Vol. 1, pp. 11-19.
[25] Lee VW, Trifunac MD. Rocking strong earthquake accelerations, Soil Dynamics and Earthquake Engineering, 1987, Vol. 6, pp. 75-89.
[26] Hong-Nan Li, Li-Ye Sun, Su-Yan Wang. Improved approach for obtaining rotational components of seismic motion, Nuclear Engineering and Design, 2004, Vol. 232, pp. 131-137.
[27] Lee VW, Liang L. Rotational components of strong motion earthquakes, The 14th World Conference on Earthquake Engineering, Beijing, China, 2008.
[28] Suryanto W, Igel H, Wassermann J, Cochard A, Schuberth B, Vollmer D, Scherbaum F, Schreiber U, Velikoseltsev A. First comparison of array-direct ring laser measurements, Bulletin of the Seismological Society of America, 2006, Vol. 96, pp. 2059-2071.
[29] Liu CC, Huang BS, Lee W, Lin CJ. Observation rotational and translational ground motion at the HGSD station in Taiwan from 2007 to 2008, Bulletin of Seismological Society of America, 2009, Vol. 99, pp. 1228-1236.
[30] Kalab Z, Knejzlik J. Example of rotational component records of mining induced seismic events from the Karvina region, Acta Geodynamica et Geomaterialia Journal, 2012, Vol. 9, No. 2, pp. 173-178.
[31] Awade AM, Humar JL. Dynamic response of buildings to ground motion, Canadian Journal of Civil Engineering, 1984, Vol. 11, pp. 48-56.
[32] Gupta VK, Trifunac MD. Investigation of buildings response to translational and rotational earthquake excitations, Report No. CE 89-02, Department of Civil Engineering, University of Southern California, 1989.
[33] Goul RK, Chopra AK. Dual-level approach for seismic design of asymmetric-plan buildings, Journal of Structural Engineering (ASCE), 1994, Vol. 120, pp. 161-179.
[34] Takeo M. Ground rotational motions recorded in near-source region of earthquakes, physical Research Letters, 1998, Vol. 25, pp. 789-792.
[35] Ghayamghamian MR, Nouri GR, Igel H, Tobita T. The effect of torsional ground motion on structural response: code recommendation for accidental eccentricity, Bulletin of the Seismological Society of America, 2009, No. 2B, Vol. 99, pp. 1261-1270.
[36] Kalani Sarokolayi L, Navayi Neya B, Tavakoli HR, Vaseghi Amiri J. Dynamic analysis of elevated water storage tanks due to ground motions' rotational and translational components, Arabian Journal of Science and Engineering, AJSE, 2012 (in press).
[37] Kalani Sarokolayi L, Navayi Neya B, Vaseghi Amiri J, Tavakoli HR. Seismic analysis of elevated water storage tanks subjected to six correlated ground motion components, Iranian Journal of Earthquake Engineering, IJEE, Iran, 2012 (in press).
[38] Kalani Sarokolayi L, Navayi Neya B, Vaseghi Amiri J, Tavakoli HR. Effect of rotational components of earthquake on dynamic response of concrete gravity dam considering reservoir interaction, Sharif Journal of Science and Technology, Iran, 2012 (in press).
[39] Clough RW, Penzien J. Dynamics of Structures, second ed, McGraw-Hill Book Company, Singapore, 1993.
[40] Navayi Neya B, Vaseghi Amiri J, Alijani Ardeshir M. A closed form solution for hydrodynamic pressure of reservoir with effect of viscosity under dynamic loading, International Conference on Civil and Engineering ICCEE, Venice, Italy, 2009.
[41] Merriam JL, Kraige LG. Engineering Mechanics-Dynamic, 6th Ed, John Wiley& Sons, 2008.
[42] Chopra AK. Earthquake behavior of reservoir-dam systems, Journal of the Engineering Mechanics Division, ASCE, 1968, No. EM6, Vol. 94, pp. 1475-1500.